Histol Histopathol (2025) 40: 1405-1413

Histology and Histopathology
From Cell Biology to Tissue Engineering

ORIGINAL ARTICLE Open Access

Assessing acute pancreatitis: A novel method combining live cell imaging with tissue damage evaluation

Polona Kovačič[1], Maša Skelin Klemen[1], Eva Paradiž Leitgeb[1], Viktória Venglovecz[2,3], Lóránd Kiss[4], Gabriella Mihalekné Fűr[4,5], Andraž Stožer[1] and Jurij Dolenšek[1,6]

[1]Institute of Physiology, Faculty of Medicine, University of Maribor, Maribor, Slovenia, [2]Department of Pharmacology and Pharmacotherapy, University of Szeged, Szeged, [3]Institute for Translational Medicine, University of Pécs, Pécs, [4]Department of Pathophysiology, University of Szeged, [5]Cancer Genomics and Epigenetics Core Group, Hungarian Centre of Excellence for Molecular Medicine (HCEMM), Szeged, Hungary and [6]Faculty of Natural Sciences and Mathematics, University of Maribor, Maribor, Slovenia

Summary. Acute pancreatitis (AP) is a sudden inflammation of the exocrine part of the pancreas, resulting in self-digestion and destruction of exocrine tissue. The intricate relationship between exocrine and endocrine functions is pivotal, as damage to acinar cells can affect endocrine cell function and *vice versa*. However, our understanding of these interactions remains limited. An effective strategy for investigating pancreatic cells involves the utilization of live *in-situ* acute mouse pancreas tissue slice preparations, combined with noninvasive fluorescent calcium labeling of endocrine or exocrine cells, and subsequent analysis using confocal laser scanning microscopy. Nevertheless, this approach encounters inherent conflicts with conventional methodologies employed to histologically assess the severity of tissue damage due to AP in the model. Traditional methods involve fixing and staining tissue samples with hematoxylin and eosin, thereby precluding live-cell imaging. In this study, our objective was to introduce an innovative method utilizing a commercial fluorescence Live/Dead assay that enables calcium imaging and tissue damage assessment in the same sample. This approach was validated against the classical histological grading of AP severity, and we found a good correlation between the classical histological grading method and the *in-situ* approach employing the Live/Dead assay. The primary advantage of our novel approach lies in its capacity to enable timely and efficient live-cell imaging together with damage assessment in the same tissue, thereby enabling the study of functional consequences of structural damage at the cellular level and reducing the number of animals required for experimentation.

Key words: Acute pancreatitis, Pancreatic tissue damage, Exocrine and endocrine interactions, Live cell imaging, Confocal laser scanning microscopy, Calcium imaging, Live/Dead assay, Tissue slice preparation, Histological grading

Corresponding Author: Jurij Dolenšek, Institute of Physiology, Faculty of Medicine, University of Maribor, Maribor, Slovenia. e-mail: jurij.dolensek@um.si

www.hh.um.es. DOI: 10.14670/HH-18-882

Introduction

Acute pancreatitis (AP) is a sudden onset inflammatory disorder of the exocrine pancreas that develops rapidly and is associated with the release of digestive enzymes into the pancreatic interstitium and into the systemic circulation, with increased production and release of cytokines, which can cause a severe local and systemic inflammatory response (Kingsnorth, 1997; Frossard et al., 2008; Kim, 2008). Most patients have mild AP, which is self-limiting and usually resolves within a week. Approximately 20% of patients develop moderate or severe AP with necrosis of pancreatic tissue, organ failure, or both, with a mortality rate of 20-40% (Boxhoorn et al., 2020). Death is more likely in certain subgroups of patients, including the elderly, those with multiple and severe comorbidities (especially obesity), patients who develop nosocomial infections, and those with severe episodes of AP (characterized by permanent failure of one or more organ systems or infected pancreatic necrosis) (Forsmark et al., 2016). Animal models are commonly used in the study of AP. Experimental induction of AP began more than a century ago to better understand the disease's pathophysiology and, potentially, to develop

targeted therapies and disease-specific treatments (Gorelick et al., 1993). One of the oldest and most often used approaches to induce AP in animal models is supraphysiological pharmacological overstimulation of acinar cells. During such stimulation, high intracellular calcium concentrations ($[Ca^{2+}]_i$) are achieved and follow non-oscillatory dynamics, which leads to pathological basolateral exocytosis, fusion of exocytotic granules with other organelles such as lysosomes, premature activation of digestive enzymes, and gland autodigestion, followed by an inflammatory response, interstitial edema, and acinar necrosis. A common and widely accepted mouse model for the induction of AP involves repeated applications of cerulein, a cholecystokinin (CCK) analog that stimulates pancreatic acinar cells to secrete digestive enzymes. Supramaximal cerulein doses lead to vacuolization within acinar cells, followed by regeneration of the pancreas; higher doses cause pancreatic interstitial edema and inflammatory cell infiltration, together with a significant increase of amylase levels in the blood. The model yields reproducible results and has strong clinical relevance, as it is the most appropriate model for the study of AP induced by organophosphate poisoning in humans (Gorelick et al., 1993; Lerch and Adler, 1994; Sah et al., 2012; Gorelick and Lerch, 2017). Many studies have predominantly utilized histology-based techniques to evaluate damage caused by AP. These methods involve measuring different types of histological damage, such as edema, leukocyte infiltration, necrosis, and vacuolization (Aho et al., 1983; Schmidt et al., 1992; Malecka-Panas et al., 2002; Moreno et al., 2006; Muftuoglu et al., 2006; Singh and Garg, 2016; Yin et al., 2017; Yang et al., 2020; Gál et al., 2021); however, these methods involve fixation of the tissue, an obligatory step in preparing sections for histological evaluation. To be able to correlate functional and structural changes during AP in the same tissue samples, a method to assess damage that is compatible with functional measurements is needed. To this end, we introduced a method in which the extent of necrosis, an essential marker of a necrotizing type of AP, is measured with a commercially available fluorescence Live/Dead assay immediately following confocal calcium imaging. We validated our approach against the gold standard, the classical histological grading of AP severity. The primary advantage of our method is its ability to perform live-cell imaging and assess tissue damage simultaneously in a quick and simple manner on the same specimens, thereby reducing biological variability and minimizing the number of animals needed for the study.

Materials and methods

Ethics statement

The study was performed in strict accordance with the criteria of national and European legislation on the protection of animals used for scientific purposes (Directive 2010/63/EU). National and European recommendations related to the care and handling of laboratory animals were strictly followed, ensuring that animal suffering was kept to an absolute minimum. The protocol of the study, which was carried out within the framework of the ARIS (Public Agency for Scientific Research and Innovation of the Republic of Slovenia) project entitled 'Effect of acute pancreatitis in a murine model on the endocrine function of the pancreas', was approved by the Food, Veterinary, and Plant Protection Administration of the Republic of Slovenia (approval number: U34401-33/2021/8, 12. 4. 2022).

Animal housing and induction of pancreatitis

We utilized two cohorts of animals using identical protocols for cerulein-induced pancreatitis: one cohort (12 male NMRI mice) dedicated to assessing pancreas viability in conjunction with live imaging of intracellular calcium concentrations, and another cohort (6 male NMRI mice) dedicated to histology-based characterization of the extent of pancreatitis (Fig. 1). Animals were housed in socially stable groups of 4 to 6 males per individually ventilated cage in conventional settings (relative humidity 45-65%, temperature 22±2°C, and 12h light cycles) and had unlimited access to water and food. The mice were randomly divided into two equally sized groups (AP and control). To reduce stress on the animals, mice were handled three times a week for two weeks prior to the start of the experimental work. Mice were fasted 6 hours before the start of the injection period in both groups. In the AP group, cerulein was injected intraperitoneally at a dose of 50 µg/kg body weight every hour for nine consecutive hours, i.e., 10 injections in total. The control group received saline injections in equal quantities at equal time intervals. To avoid unnecessary suffering and agony, 540 g/kg of metamizole, an analgesic, antispasmodic, and antipyretic, was administered intraperitoneally at the fourth and tenth injections of cerulein/saline in both groups of animals.

Assessing pancreatic viability in conjunction with live intracellular calcium imaging

Acute pancreas tissue slices were prepared as described previously (Speier and Rupnik, 2003; Stožer et al., 2021a). Animals were sacrificed by exposure to excessive CO_2 concentrations and cervical dislocation. To access the abdominal cavity, a V-shaped laparotomy was performed and the common bile duct was exposed. The pancreas was injected with 1.9% low-melting-point agarose (Lonza Bioscience, Basel, Switzerland) at the proximal common bile duct. Prior to injection, agarose was dissolved in extracellular solution (ECS) containing (in mM) 125 NaCl, 2.5 KCl, 26 $NaHCO_3$, 1.25 NaH_2PO_4, 2 Na-pyruvate, 0.25 ascorbic acid, 3 myo-inositol, 1 $MgCl_2$, 2 $CaCl_2$, 6 lactic acid, 6 glucose, bubbled with carbogen and kept in a prewarmed water bath at 40°C. To prevent agarose from passing into the duodenum during retrograde injection, the duodenal

papillae (papilla of Vater), which connects the hepatic and biliary ducts, was clamped using a folded hemostat. Following the agarose injection, the abdominal cavity was immediately cooled with ice-cold ECS. The pancreas was excised and placed in ice-cold ECS. After removing the connective and adipose tissue, the pancreas was cut into smaller pieces. These were then embedded in agarose and sliced into 140-µm-thick sections using a vibratome (VT 1000 S, Leica) in ice-cold ECS. Slices were transferred into HEPES-buffered saline (HBS, consisting of (in mM) 150 NaCl, 10 HEPES, 6 glucose, 5 KCl, 2 $CaCl_2$, 1 $MgCl_2$; titrated to pH=7.4 with 1 M NaOH) at room temperature. For calcium-reported dye loading, the slices were incubated in a solution containing 6.86 µM Calbryte 520 AM (AAT Bioquest, Pleasanton, CA, USA), 0.11% dimethylsulfoxide (DMSO), and 0.037% Pluronic F-127 (20% stock solution in DMSO) at room temperature for 50 min. If not specified otherwise, all chemicals were obtained from Sigma Aldrich (St. Louis, MO, USA). Individual tissue slices were subjected to confocal calcium imaging as described in Stožer et al. (2013, 2021a) and Pohorec et al. (2022). Immediately thereafter, we assessed the viability of cells within the slices using a Live/Dead Viability/Cytotoxicity Kit (Invitrogen, Thermo Fisher Scientific, Waltham, USA) according to the manufacturer's protocol and as described previously (Stožer et al., 2021a). In brief, slices were incubated in a solution containing 2 µM calcein AM (solution A) and 4 µM ethidium homodimer-1 (solution B) in PBS at room temperature for 30-45 minutes. Imaging of cell viability was carried out using a Leica STELLARIS SP8 FALCON DIVE upright

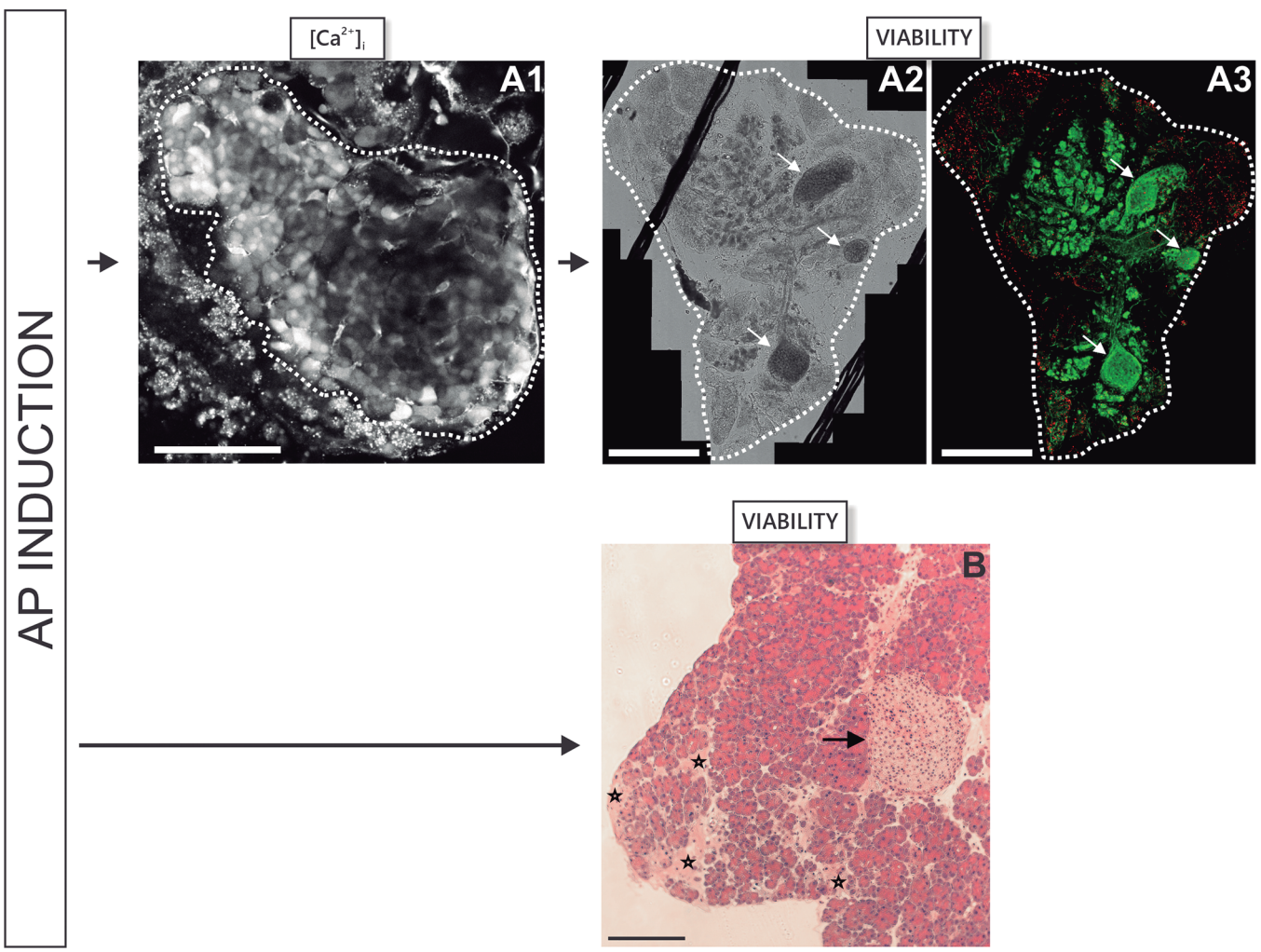

Fig. 1. Experimental design. **A.** Following induction of acute pancreatitis (AP) by cerulein, acute pancreas tissue slices were stained with $[Ca^{2+}]_i$ reporter dye (**A1**, outlined is an islet of Langerhans) and used for confocal $[Ca^{2+}]_i$ imaging; subsequently, the same slice was stained with Live/Dead assay (**A2**, demonstrated transmission confocal image with islets indicated with arrows, **A3**, false colors: green - live cells and red - nuclei of dead cells with islets indicated with arrows) to assess the viability of the tissue. **B.** Following the same protocol for AP induction in a separate cohort of animals, thin sections of pancreas were used for histological characterization. Asterisks denote necrotic areas and the arrow points *to an islet*. Scale bars: A1, B, 100 μm; A2, A3, 500 μm

confocal system (objective: 20x water immersion, HC APO L U-V-I, NA 0.9), with excitation set at 495 nm, and the emitted fluorescence collected with a Leica HyD detector at 500-555 (calcein AM) and at 625-695 nm (ethidium homodimer-1) alongside a transmitted confocal image using a PMT detector. Z-stack of large areas covering exo- and endocrine tissue over multiple fields of vision were obtained. Offline, we used Fiji, an open-source image processing package based on ImageJ, to perform maximal projection in the z-direction and visually select areas that were positive for the green and red emission channels. We manually selected areas populated by red and green channels and calculated the fraction of dead areas using the equation:

$$\text{fraction} = \frac{\text{Ch}_\text{R}}{\text{Ch}_\text{G} + \text{Ch}_\text{R}}$$

in which Ch_R denotes the area of the red and Ch_G the area of the green channel. To enhance the visibility of the red and green channels, we applied Flat Field correction, gamma adjustment, and brightness enhancement to the original recordings using Fiji.

Assessing pancreatic viability using histological staining

Animals were sacrificed as described in the section above. The tissue was fixed in paraformaldehyde (PFA) and glutaraldehyde (GA), embedded in paraffin wax, and sectioned into 3-µm-thick slices. The slices were then stained with hematoxylin-eosin following standard protocols (Cardiff et al., 2014). Three examiners double-blindly evaluated histological slices separately and independently. Four different types of tissue characteristics due to AP (edema, leukocyte infiltration, necrosis, and vacuolization) were assessed in 96 sections prepared from four different parts of the pancreas (duodenal, gastric, proximal splenic, and distal splenic) of six mice (three from the control group (CTRL) and three from the acute pancreatitis group (AP)). The edema, leukocyte infiltration, necrosis, and vacuolization

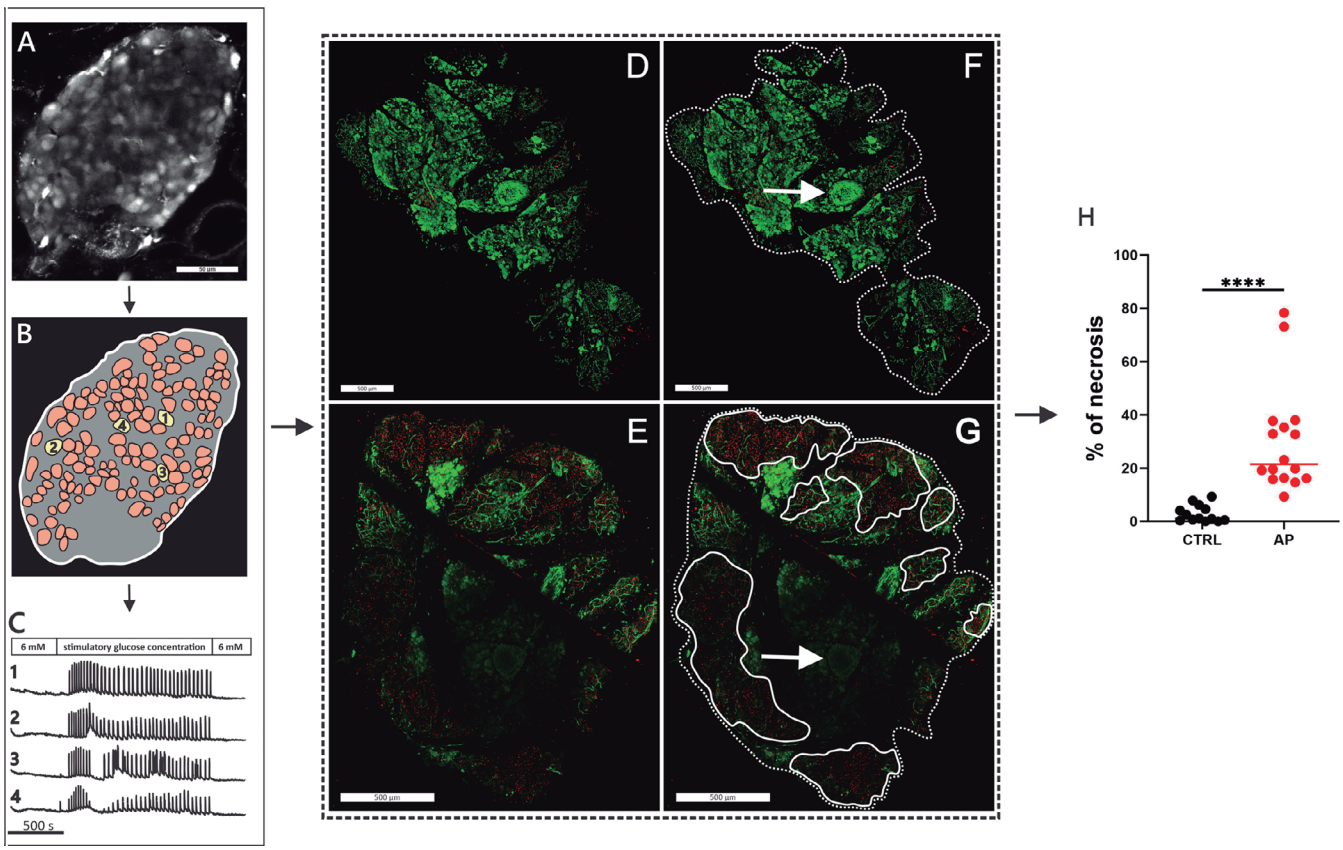

Fig. 2. Assessing $[Ca^{2+}]_i$ activity and cell viability in acute pancreas tissue slices. **A-C.** Acute pancreas slices were stained with $[Ca^{2+}]_i$ reporter dye (**A**, shown is an islet with surrounding acinar tissue). Individual endocrine cells were outlined **(B)**, and $[Ca^{2+}]_i$ activity following glucose stimulation measured (**C**, protocol for stimulatory glucose concentration indicated). **D-G.** The same slices were imaged using a Live/Dead assay, displaying green fluorescence from the cytoplasm of live cells and red fluorescence from nuclei of dead cells in the control **(D)** and cerulein-induced-AP **(E)** groups. Areas dominated by the red (solid line) and green (dotted line) channels are outlined for the slices in panels **F** and **G**; arrows point to an islet. **H.** Relative proportion of areas dominated by the red channel from control (black) and cerulein-induced-AP (red) groups. The median value is depicted by a line. Pooled data from 12 animals and 23 slices. AP: acute pancreatitis, CTRL: control. ****p<0.0001 (Mann-Whitney U test). Scale bars: A, 50 μm; D-G, 500 μm.

were separately graded on the scale presented in Table 1 for each type of injury. We calculated the median scores of each assessor according to the parameter measured and the part of the pancreas. To enhance contrast, we subtracted the background and applied gamma correction to the histological slices using Fiji.

Results

We developed and validated a method that allows for the quantification of pancreatitis in pancreas tissue slices subsequent to imaging live cell $[Ca^{2+}]_i$ activity. In the first step, acute pancreas tissue slices were prepared and subjected to confocal $[Ca^{2+}]_i$ imaging of endocrine, acinar, and ductal cells as described elsewhere (Speier and Rupnik, 2003; Dolenšek et al., 2013; Stožer et al., 2013, 2021a,b; Gál et al., 2019; Sluga et al., 2021; Marolt et al., 2022) (Fig. 2). The cell activity data can be analyzed offline and were not further analyzed for the purpose of this paper. In the next step, immediately after $[Ca^{2+}]_i$ imaging, individual slices were stained using a commercially available Live/Dead kit (Fig. 2). The kit discriminated live from dead cells: one component (calcein AM) stained live cells with bright fluorescence in the green spectrum, whereas the other component (ethidium homodimer-1) stained nuclei from cells with disintegrated membranes (designated as dead cells) with bright fluorescence in the red spectrum. In the acinar tissue from the AP group, we observed distinct areas that contained either predominantly red or predominantly green emissions with superficial nuclei in the red channel (Fig. 2E,G). In the control group, the red-dominated areas were scarce and limited to tissue slice edges (Fig. 2D,F). Islets of Langerhans were visible in the green channel and contained minor superficial red nuclei in both groups (Fig. 2D-G). As a measure of the proportion of necrotic areas, we quantified the relative surface of red-dominated areas for individual slices and displayed pooled data in Figure 2H. AP induction was characterized by a statistically significant increase in the proportion of necrotic areas from a median 1.1% (interquartile range (IQR) = 5.0%) in the control group to a median 21.5% (IQR = 20.9%) in the AP group.

In the next step, we validated the method by comparing the above result with a gold-standard method based on a scoring system of histological sections (Table 1). We quantified the extent of necrosis, as well as edema, leukocyte infiltration, and vacuolization on hematoxylin-eosin-stained pancreas sections (Fig. 3). The extent of edema was significantly increased in the AP group (median = 0.5 and 2, IQR = 1 and 1 for the control and AP group, respectively). Similarly, increased levels of leukocyte infiltration were observed in the AP group (median = 0 and 2, IQR = 0 and 1 for the control and AP group, respectively). Additionally, a significant rise in the degree of vacuolization was observed in the AP group (median = 0 and 2, IQR = 0 and 0.75 for the control and AP group, respectively). Most importantly, the AP group exhibited a marked increase in the relative proportion of necrotic areas (median = 5 and 30%, IQR = 10 and 25%, respectively).

To validate the method, we compared the extent of necrosis obtained from live tissue slices with histological sections (Fig. 4). As presented above, both approaches reported a statistically significant increase in the proportion of necrotic areas following cerulein-induced AP (median = 21.5% and 30%, IQR = 20.9% and 25% by the Live/Dead method and by the scoring method, respectively) compared with the control group (median = 1.1% and 5%, IQR = 5% and 10% by the Live/Dead method and by the scoring method, respectively). Most importantly, there was no statistically significant difference in the proportion of necrotic areas assessed by both methods, either within the control or the AP group.

Discussion

AP has many consequences long after clinical resolution and should no longer be considered a self-limiting disease. AP can progress rapidly and cause severe symptoms, such as a systemic inflammatory response, which can lead to multiple outcomes and predispose patients to develop diabetes of the exocrine pancreas (Lankisch et al., 2015). Although there has been progress in understanding the pathophysiology of AP through animal models (Singh and Garg, 2016; Gorelick and Lerch, 2017; Yang et al., 2020), our knowledge regarding the underlying mechanisms by which AP impacts the endocrine pancreas remains limited (Malecka-Panas et al., 2002; Gál et al., 2021). This underscores the critical need for focused research in this area. Numerous studies have primarily employed histology-based approaches to assess damage due to AP (Anderson et al., 1969; Aho et al., 1983; Tani et al., 1987; Schmidt et al., 1992; Laethem et al., 1998; Moreno et al., 2006; Muftuoglu et al., 2006; Ouziel et

Table 1. Scoring system for the evaluation of pancreatic injury in histological sections.

	Scores	0	1	2	3	4
Instertitial edema	0-3	Not present	Inconsistently scattered between the lobules	Diffuse interlobular	Interlobular and intralobular (interacinar)	-
Leukocyte infiltration	0-4	Not present	Focal	Diffuse/mild	Diffuse/moderate	Diffuse/severe
Necrosis	%	-	-	-	-	-
Vacuolization	0-3	Not present	Diffuse/mild	Diffuse/moderate	Diffuse/severe	-

al., 2012; Yin et al., 2017). These methods are based on evaluating various types of histological damage, including edema, leukocyte infiltration, necrosis, and vacuolization. A skilled analyst is needed to detect and discriminate histological changes, such as separation of lobules and acini due to edematous fluid in the

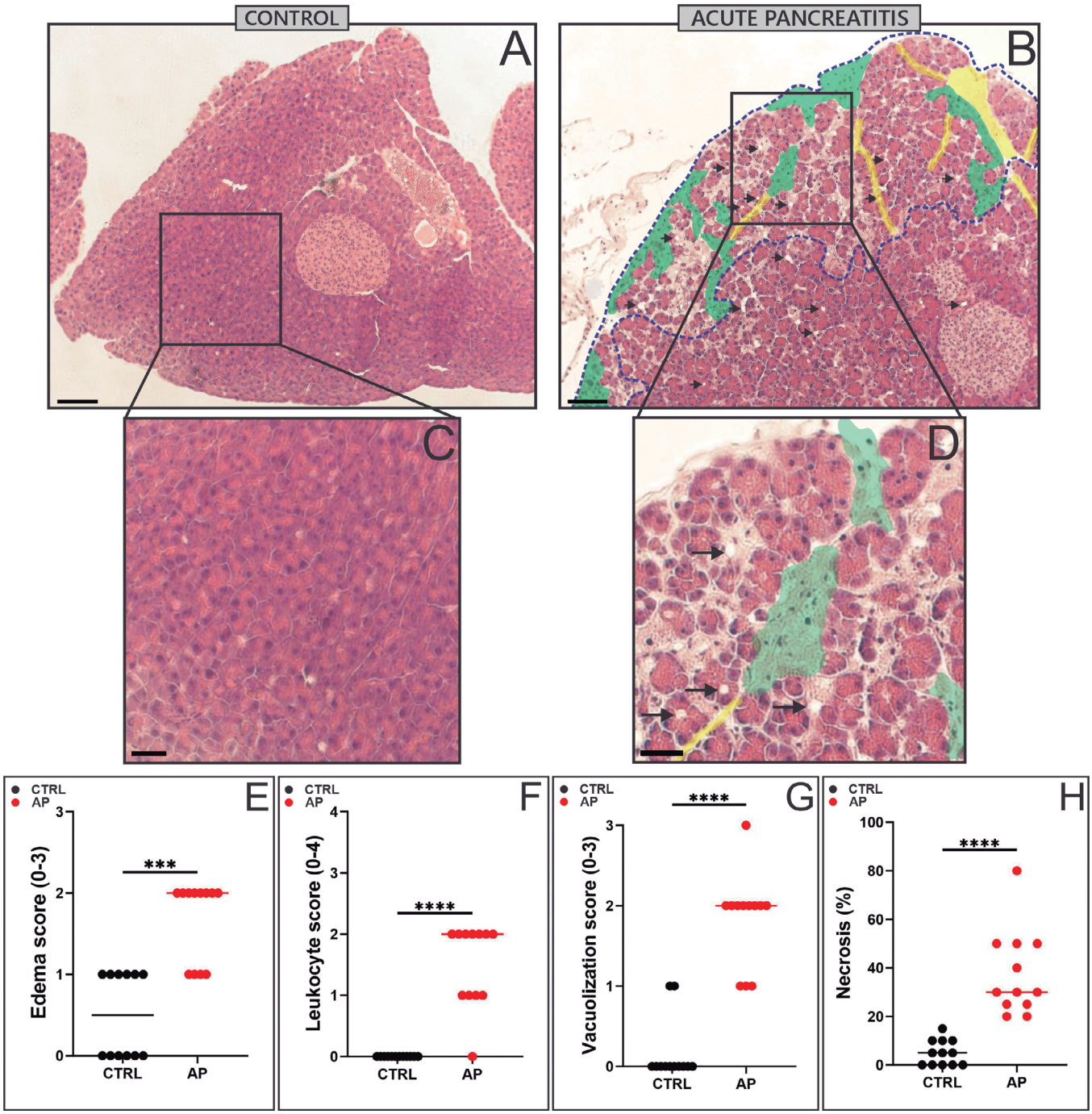

Fig. 3. Characterization of cerulein-induced AP using a grading system on histological sections. **A-D.** Hematoxylin-eosin-stained pancreatic sections from a control (**A**, zoomed portion in panel **C**) and AP (**B**, zoomed portion in panel **D**) animal. Yellow overlay denotes edema, green overlay leukocyte infiltration, arrows vacuoles, and blue dotted line encircled necrotic area. **E-H.** A double-blinded scoring system was used to assess the extent of edema **(E)**, leukocyte infiltration **(F)**, vacuolization **(G)**, and necrosis **(H)** in the control (black) and AP-induced (red) groups. ***$p<0.001$, ****$p<0.0001$ (Mann-Whitney U test). Scale bars: A, B, 100 μm; C, D, 500 μm.

extracellular space in the case of edema; altered basophilic staining or deranged cellular organization in the case of necrosis; the presence of vacuoles within the cytoplasm, or leukocytes within the acinar interstitial spaces (Nevalainen and Aho, 1992; Kui et al., 2015; Yin et al., 2017). Quantification is classically based on either assigning scored values to morphological changes (Anderson et al., 1969; Schmidt et al., 1992; Laethem et al., 1998; Moreno et al., 2006; Muftuoglu et al., 2006; Ouziel et al., 2012) or measuring the proportion of necrotic tissue in the total lobular parenchyma (Aho et al., 1983). The scoring system is suitable for evaluating both edematous and necrotizing pancreatitis, while the histometric measurement of necrotic parenchyma is applicable only in cases of necrotizing experimental pancreatitis (Nevalainen and Aho, 1992). Although the scoring system is considered the golden standard method to study AP, this approach is inherently limited due to tissue fixation during histology preparation. This step prevents a direct correlation between histology and function on the level of the same animal or the same tissue. Therefore, separate animal cohorts have typically been used for histological and functional assessments (Kinami et al., 1982). This is noteworthy, as animals express some differences in the extent of tissue damage, even if an identical protocol for pancreatitis induction is used (Niederau et al., 1985; Seifert et al., 2017); this may impose considerable bias when correlating changes in function with structural changes. Moreover, heterogeneity in responsiveness of exo- (Yule et al., 1991; Marolt et al., 2022) and endocrine cells (Van Schravendijkz et al., 1992; Pipeleers et al., 1994; Stožer et al., 2021b) may further (Nevalainen and Aho, 1992; Kui et al., 2015) mask functional changes if data are not correlated from the same tissue. Monitoring function using confocal imaging of $[Ca^{2+}]_i$ changes, although employed with much success in endo- (Asada et al., 1998; Stožer et al., 2013a,b, 2021b; Pohorec et al., 2022, 2023;) and exocrine cells (Niederau et al., 1985; Seifert et al., 2017; Gál et al., 2021; Marolt et al., 2022), does not report cells that completely lack activity and this may add to the methodological bias when characterization is based solely on functional imaging. An appealing approach thus seems to be to perform post-imaging tissue slice fixation, followed by further sectioning from typical 140-µm tissue slices to typical 5-µm semithin sections suitable for histology analysis; however, this is an extremely tedious and time-consuming approach to perform. We therefore sought to develop an approach that would simplify the method and make it generally more appealing to researchers. To this end, we measured the viability of acute pancreas slices using a commercially available Live/Dead kit immediately following live cell calcium imaging, circumventing the need for fixation and resectioning, and validated this approach against the gold standard scoring system on histological sections. Both methods reported similar results, i.e., an identical proportion of necrotic areas under control conditions and a comparable increase in the proportion of necrotic areas due to cerulein induction (Fig. 4). Thus, our proposed method is a promising alternative to histological assessment whenever live cell calcium imaging or some other assay of cell function (such as electrophysiological or secretion measurements) is required to determine the relationship between functional and structural changes on the same tissue sample. We would like to acknowledge that, in its current form, our method is limited to necrotizing-type pancreatitis, and a classical histological approach would still be needed in other types of pancreatitis. At least theoretically, in tissue slices, the size of intercellular, interacinar, and interlobular spaces can be quantified using extracellular fluorescent polar dyes (such as sulforhodamine B) (Low et al., 2014), intracellular vacuoles can be visualized with the help of dextran-bound indicators (Voronina et al., 2007), and leukocytes can be visualized using genetically encoded Ca^{2+} indicators (Weitz et al., 2018). In the future, employing some of these approaches in addition to the Live/Dead assay should enable researchers to better quantify the function-structure relationship in live pancreas tissue under different types of pancreatitis and other diseases.

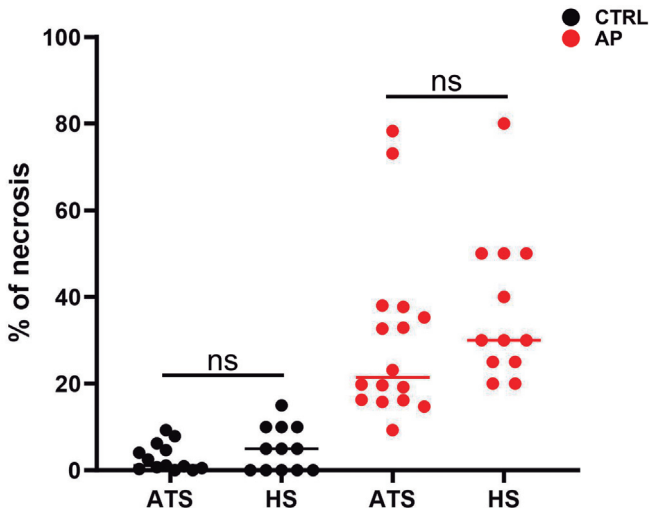

Fig. 4. Comparison of the two methods. The extent of necrosis measured from acute tissue slices (ATS) and histological section (HS) in the control (black) and AP (black) group. Data from Figures 2-3. Mann-Whitney U test, ns: non-significant differences in medians.

Acknowledgements. We thank Rudi Mlakar, Jasmina Jakopiček, and Maruša Plesnik Rošer for their excellent technical assistance.

Funding. The work presented in this study was financially supported by the Slovenian Research Agency Programs I0-0029 and P3-0396, and projects J3-9289, N3-0133, N3-0170, and J3-3077, as well as by the National Research, Development and Innovation Office (SNN134497 to VV).

References

Aho H.J., Nevalainen T.J. and Aho A.J. (1983). Experimental pancreatitis in the rat. Development of pancreatic necrosis, ischemia and edema after intraductal Sodium taurocholate injection. Eur. Surg. Res. 15, 28-36.

Anderson M.C., Needleman S.B., Gramatica L., Richard Toranto I. and Briggs D.R. (1969). Further inquiry into the pathogenesis of acute pancreatitis: Role of pancreatic enzymes. Arch. Surg. 99, 185-192.

Asada N., Shibuya I., Iwanaga T., Niwa K. and Kanno T. (1998). Identification of alpha- and beta-cells in intact isolated islets of Langerhans by their characteristic cytoplasmic Ca^{2+} concentration dynamics and immunocytochemical staining. Diabetes 47, 751-757.

Boxhoorn L., Voermans R.P., Bouwense S.A., Bruno M.J., Verdonk R.C., Boermeester M.A., van Santvoort H.C. and Besselink M.G. (2020). Acute pancreatitis. Lancet 396, 726-734.

Cardiff R.D., Miller C.H. and Munn R.J. (2014). Manual hematoxylin and eosin staining of mouse tissue sections. Cold Spring Harb. Protoc. 6, 655-658.

Dolenšek J., Stožer A., Klemen M.S., Miller E.W., and Rupnik M.S. (2013). The relationship between membrane potential and calcium dynamics in glucose-stimulated beta cell syncytium in acute mouse pancreas tissue slices. PLoS One 8, e82374.

Forsmark C.E., Swaroop Vege S. and Wilcox C.M. (2016). Acute pancreatitis. N. Engl. J. Med. 375, 1972-1981.

Frossard J.L., Steer M.L. and Pastor C.M. (2008). Acute pancreatitis. Lancet 371, 143-152.

Gál E., Dolenšek J., Stožer A., Pohorec V., Ébert A. and Venglovecz V. (2019). A novel *in situ* approach to studying pancreatic ducts in mice. Front. Physiol. 10, 938.

Gál E., Dolenšek J., Stožer A., Czakó L., Ébert A. and Venglovecz V. (2021). Mechanisms of post-pancreatitis diabetes mellitus and cystic fibrosis-related diabetes: A review of preclinical studies. Front. Endocrinol. 12, 715043.

Gorelick F.S., Adler G. and Kern H.F. (1993). Cerulein-induced pancreatitis. In: The pancreas: Biology, pathobiology, and disease, Second edition. Raven Press, Ltd.. New York. pp 501-526.

Kim H. (2008). Cerulein pancreatitis: Oxidative stress, inflammation, and apoptosis. Gut Liver 2, 74-80.

Kinami Y., Mura T., Sugii M. and Miyazaki I. (1982). Function of pancreatic endocrine cells in experimental acute pancreatitis. World J. Surg. 6, 471-477.

Kingsnorth A. (1997). Role of cytokines and their inhibitors in acute pancreatitis. Gut 40, 1-4.

Kui B., Balla Z., Vasas B., Végh E.T., Pallagi P., Kormányos E.S., Venglovecz V., Iványi B., Takács T., Hegyi P. and Rakonczay Z. (2015). New insights into the methodology of L-arginine-induced acute pancreatitis. PLoS One 10, e0117588.

Laethem J.L. Van, Eskinazi R., Louis H., Rickaert F., Robberecht P. and Devière J. (1998). Multisystemic production of interleukin 10 limits the severity of acute pancreatitis in mice. Gut 43, 408-413.

Lankisch P.G., Apte M. and Banks P.A. (2015). Acute pancreatitis. Lancet 386, 85-96.

Lerch M.M. and Adler G. (1994). Pathophysiology of acute pancreatitis. Dig. Surg. 11, 186-192.

Low J.T., Zavortink M., Mitchell J.M., Gan W.J., Do O.H., Schwiening C.J., Gaisano H.Y. and Thorn P. (2014). Insulin secretion from beta cells in intact mouse islets is targeted towards the vasculature. Diabetologia 57, 1655-1663.

Malecka-Panas E., Gasiorowska A. and Mokrowiecka A. (2002). Endocrine pancreatic function in patients after acute pancreatitis. Hepatogastroenterology 49, 1707-1712.

Marolt U., Leitgeb E.P., Pohorec V., Lipovšek S., Venglovecz V., Gál E., Ébert A., Menyhárt I., Potrč S., Gosak M., Dolenšek J. and Stožer A. (2022). Calcium imaging in intact mouse acinar cells in acute pancreas tissue slices. PLoS One 17, e0268644.

Moreno C., Nicaise C., Gustot T., Quertinmont E., Nagy N., Parmentier M., Louis H., Devière J. and Deviè J. (2006). Chemokine receptor CCR5 deficiency exacerbates cerulein-induced acute pancreatitis in mice. Am. J. Physiol. Gastrointest. Liver Physiol. 291, 1089-1099.

Muftuoglu M.A.T., Isikgor S., Tosun S. and Saglam A. (2006). Effects of probiotics on the severity of experimental acute pancreatitis. Eur. J. Clin. Nutr. 60, 464-468.

Nevalainen T.J. and Aho H.J. (1992). Standards of morphological evaluation and histological grading in experimental acute pancreatitis. Eur. Surg. Res. 24, 14-23.

Niederau C., Ferrell L.D., and Grendell J.H. (1985). Caerulein-induced acute necrotizing pancreatitis in mice: Protective effects of proglumide benzotript, and secretin. Gastroenterology 88, 1192-1204.

Ouziel R., Gustot T., Moreno C., Arvanitakis M., Degré D., Trépo E., Quertinmont E., Vercruysse V., Demetter P., Le Moine O., McKenzie A.N.J., Delhaye M., Devière J. and Lemmers A. (2012). The ST2 pathway is involved in acute pancreatitis: A translational study in humans and mice. Am. J. Pathol. 180, 2330-2339.

Pipeleers D., Kiekens R., Ling Z., Wilikens A. and Schuit F. (1994). Physiologic relevance of heterogeneity in the pancreatic beta-cell population. Diabetologia 37, S57-S64.

Pohorec V., Križančić Bombek L., Skelin Klemen M., Dolenšek J. and Stožer A. (2022). Glucose-stimulated calcium dynamics in beta cells from male C57BL/6J, C57BL/6N, and NMRI mice: A comparison of activation, activity, and deactivation properties in tissue slices. Front. Endocrinol. 13, 867663.

Pohorec V., Zadravec N., Turk M., Dolenšek J. and Stožer A. (2023). Alpha cell stimulus-secretion coupling and intercellular interactions in health and type 2 diabetes. Acta Medico-Biotechnica 16, 21-28.

Sah R.P., Garg P. and Saluja A.K. (2012). Pathogenic mechanisms of acute pancreatitis. Curr. Opin. Gastroenterol. 28, 507-515.

Schmidt J., Lewandrowski K., Fernandez-del Castillo C., Mandavilli U., Compton C., Warshaw A. and Rati D. (1992). Histopathologic correlates of serum amylase activity in acute experimental pancreatitis. Dig. Dis. Sci. 37, 1426-1433.

Seifert G.J., Sander K.C., Richter S. and Wittel U.A. (2017). Murine genotype impacts pancreatitis severity and systemic inflammation: An experimental study. Ann. Med. Surg. 24, 8-14.

Singh P. and Garg P.K. (2016). Pathophysiological mechanisms in acute pancreatitis: Current understanding. Indian J. Gastroenterol. 35, 153-166.

Sluga N., Postić S., Sarikas S., Huang Y.C., Stožer A. and Slak R.M. (2021). Dual mode of action of acetylcholine on cytosolic calcium oscillations in pancreatic beta and acinar cells *in situ*. Cells 10, 1580.

Speier S. and Rupnik M. (2003). A novel approach to *in situ* characterization of pancreatic β-cells. Pflugers. Arch. Eur. J. Physiol. 446, 553-558.

Stožer A., Dolenšek J. and Rupnik M.S. (2013a). Glucose-Stimulated calcium dynamics in islets of langerhans in acute mouse pancreas tissue slices. PLoS One 8, e54638.

Stožer A., Dolenšek J., Skelin Klemen M. and Slak Rupnik M. (2013b). Cell physiology in tissue slices studying beta cells in the islets of langerhans. Acta Medico-Biotechnica 6, 20-32.

Stožer A., Dolenšek J., Bombek L.K., Pohorec V., Rupnik M.S. and Klemen M.S. (2021a). Confocal laser scanning microscopy of calcium dynamics in acute mouse pancreatic tissue slices. J. Vis. Exp. 170, e62293.

Stožer A., Klemen M.S., Gosak M., Bombek L.K., Pohorec V., Rupnik M.S. and Dolenšek J. (2021b). Glucose-dependent activation, activity, and deactivation of beta cell networks in acute mouse pancreas tissue slices. Am. J. Physiol. Endocrinol. Metab. 321, 305-323.

Tani S., Otsuki M., Ltoh H., Fujii M., Nakamura T., Oka T., Baba S. and Otsuki M. (1987). Histologic and biochemical alterations in experimental acute pancreatitis induced by supramaximal caerulein stimulation. Int. J. Pancreatol. 2, 337-348.

Van Schravendijkz C.F.H., Kiekens R., and Pipeleers D.G. (1992). Pancreatic beta cell heterogeneity in glucose-induced insulin secretion. J. Biol. Chem. 267, 21344-21348.

Voronina S.G., Sherwood M.W., Gerasimenko O.V, Petersen O.H. and Tepikin A.V. (2007). Innovative methodology visualizing formation and dynamics of vacuoles in living cells using contrasting dextran-bound indicator: endocytic and nonendocytic vacuoles. Am. J. Physiol. Gastrointest. Liver Physiol. 293, 1333-1338.

Weitz J.R., Makhmutova M., Almaça J., Stertmann J., Aamodt K., Brissova M., Speier S., Rodriguez-Diaz R. and Caicedo A. (2018). Mouse pancreatic islet macrophages use locally released ATP to monitor beta cell activity. Diabetologia 61, 182-192.

Yang X., Yao L., Fu X., Mukherjee R., Xia Q., Jakubowska M.A., Ferdek P.E., and Huang W. (2020). Experimental acute pancreatitis models: History, current status, and role in translational research. Front. Physiol. 11, 614591.

Yin T., Peeters R., Liu Y., Feng Y., Zhang X., Jiang Y., Yu J., Dymarkowski S., Himmelreich U., Oyen R. and Ni Y. (2017). Visualization, quantification and characterization of caerulein-induced acute pancreatitis in rats by 3.0T clinical MRI, biochemistry and histomorphology. Theranostics 7, 285-294.

Yule D.I., Lawrie A.M. and Gallacher D.V. (1991). Acetylcholine and cholecystokinin induce different patterns of oscillating calcium signals in pancreatic acinar cells. Cell Calcium 12, 145-151.

Accepted February 4, 2025